

**Multislit interference patterns in high-order harmonic generation in C<sub>60</sub>**

M. F. Ciappina and A. Becker

*Max-Planck-Institut für Physik komplexer Systeme, Nöthnitzer Strasse 38, D-01187 Dresden, Germany*

A. Jaroń-Becker

*Institut für Physikalische Chemie und Elektrochemie, Technische Universität Dresden, D-01062 Dresden, Germany*

(Received 24 October 2007; published 14 December 2007)

We study high-order harmonic generation in C<sub>60</sub> molecules interacting with a linearly polarized intense short laser pulse at near- and mid-infrared wavelengths, using an extension of the so-called three-step or Lewenstein model to the molecular case. The results exhibit modulations in the plateaus of the spectra at the longer wavelengths, which are present for ensembles of aligned as well as randomly oriented fullerenes. The analysis of the results show that the minima can be explained by a multislit interference effect arising from the contributions of the 60 atomic centers to the dipole moment. Good agreement between the positions of the minima in the spectra obtained in the length gauge are found with those of the recombination matrix element, but not for those in the velocity gauge calculations. We further use a simple spherical model to analyze how geometrical information, such as the radius of the fullerene cage, can be obtained from the interference pattern in the harmonic spectra.

DOI: [10.1103/PhysRevA.76.063406](https://doi.org/10.1103/PhysRevA.76.063406)

PACS number(s): 33.80.Rv, 33.80.Wz, 42.50.Hz

**I. INTRODUCTION**

One of the exciting goals in intense laser science is that of imaging dynamical changes in molecular structure and molecular reactions on an ultrafast time scale. In laser femtochemistry, the investigation of chemical reactions using femtosecond laser pulses is a well-established area [1]. Due to the multicenter nature of the molecular species, intense field phenomena associated with the microscopic response to the radiation can contain information about the molecular structure, even on a (sub)femtosecond time scale. One of the promising tools for such investigations is high-harmonic generation (HHG) (for a recent review, see [2]). This perspective becomes obvious from the physical mechanism behind HHG, as it is has been established in the so-called three-step model [3,4]: The first step is the strong-field ionization of the atom or molecule as a consequence of the nonperturbative interaction with the coherent electromagnetic radiation. The classical propagation of the electron in the field defines the second step of the model. Finally, the third step in the sequence occurs when the electron is steered back in the linearly polarized field to its origin, recombining under the emission of a high-energy photon. One of the main features of the HHG process is the coherence of the emitted radiation, which, e.g., opens the possibility of generating attosecond pulses [5]. Another unique aspect of HHG is its sensitivity to the orientation and structure of the molecule and the symmetry of the highest occupied molecular orbital (HOMO) [6,7]. It is due to interferences arising between the dipole amplitudes from the atomic centers in the molecule, leading to minima in the high-harmonic spectrum, as has been shown both theoretically [6,8,9] and experimentally [10–12]. The potential of the process for a tomographic reconstruction of the active molecular orbital from HHG spectra is a matter of active debate [13–20].

Both the ionization and the recombination steps in HHG depend, in general, on the structure (positions of the nuclei and orbital symmetries) as well as the orientation of the mol-

ecule. This has been shown for diatomic molecules, such as H<sub>2</sub> [6,8,9] and N<sub>2</sub> [13], the triatomic molecule CO<sub>2</sub> [10,11], and, very recently, for polyatomic molecular species [12]. A general feature of all these studies is that, even for retrieval of information about the atomic frame of the molecule alone, it is necessary to align the molecular sample in the experiment. For ensembles of randomly oriented molecules, the distinct interference signatures in the HHG spectrum get smeared out and disappear. The condition of alignment is expected to hold for most of the molecules, with the potential exception of those with a highly symmetric atomic frame. The fullerenes, composed of carbon atoms, form a group with the latter characteristic feature, C<sub>60</sub> being the most prominent example among them.

It has been shown in the past that geometric properties of the atomic cage and interference effects play a relevant role in the response of C<sub>60</sub> to weak and strong electromagnetic fields. One such process is photoionization by weak synchrotron radiation. Measurements of the photoionization cross sections of the two highest occupied molecular orbitals, i.e., the HOMO and HOMO–1, as a function of the photon energy have revealed oscillations in the photon energy range above 20 eV [21–25]. These observations have been attributed [24,26] to geometrical properties of the fullerene, such as its diameter and the thickness of the electron shell. Furthermore, in a recent theoretical analysis of the saturation intensities of C<sub>60</sub> and its ions, it has been shown [27,28] that a multislit interference effect between partial waves emitted from the different C atoms of the fullerene leads to a suppression of the ionization probability of such molecules in a strong laser field. Consequently, fullerenes are harder to ionize as compared to a companion atom having the same ionization potential. It is the goal of the present paper to investigate whether or not this multislit interference effect leaves its footprints on the HHG spectrum of a randomly oriented ensemble of C<sub>60</sub> molecules.

HHG in complex molecules represents a challenge from the computational point of view. *Ab initio* calculations based

on the numerical integration of the time-dependent Schrödinger equation are possible nowadays for small diatomic molecules only, e.g.,  $\text{H}_2^+$  [8,29–34]. An alternative is the application of the strong-field approximation (SFA) for HHG, as has been proposed by Lewenstein *et al.* [35]. Since computations within this model take much less computational effort than *ab initio* simulations, it is particularly useful for studies in complex molecules, such as  $\text{C}_{60}$ .

The Lewenstein model was originally proposed for HHG in atoms [35]. In this approach the time-dependent dipole moment for an atom in an intense laser field is evaluated by considering a transition of the atom from its ground state to the Volkov states. The Lewenstein model makes use of the so-called single active electron (SAE) approximation, in which it is assumed that just one electron becomes active during the response to the external field. Furthermore, transitions to excited bound states as well as the Coulomb interaction of the electron with the ion in the continuum are neglected.

The extension of the Lewenstein model to the molecular case is currently discussed (e.g., [36,37]). Of course, a molecular ground-state wave function, which takes account of the positions of the nuclei and the symmetry of the active orbital, has to be considered. The orbital can be, e.g., approximated as a linear combination of atomic orbitals (LCAO) using quantum chemical structure programs. In the length gauge, as was originally used in the Lewenstein model, the breakdown of the translational invariance of the SFA [38] may lead to unphysical results. For example, in the case of diatomic molecules with large internuclear distances an extension of the cutoff of the high-harmonic spectrum beyond the semiclassical limit of  $3.17U_p + I_p$  has been found in numerical calculations [36]. Here,  $U_p = I/4\omega^2$  is the quiver energy of a free electron in a laser field of intensity  $I$  and frequency  $\omega$ , and  $I_p$  is the ionization potential of the molecule. It is expected [36] that such effects do occur for internuclear distances  $R > 2\alpha_0$ , where  $\alpha_0 = E/\omega^2$  is the quiver radius of the electron and  $E$  is the field strength. For a Ti:sapphire laser system operating at 800 nm and intensities of the order of  $5 \times 10^{13}$  W/cm<sup>2</sup>, the quiver radius is of the order of 10 a.u., which indicates that at these typical laser parameters the above findings would apply for diatomics with  $R \approx 20$  a.u. and larger. Although this estimation is done for diatomics, we may adopt it to the fullerene case. The diameter of the  $\text{C}_{60}$  fullerene and, hence, the largest internuclear distance between two carbon atoms in the fullerene, is about 13.4 a.u., which leads us to expect that the length gauge formalism can be used in this particular case. On the other hand, the problem of the breakdown of the translational invariance can be circumvented by using the velocity gauge [36] or, for diatomic molecules, by considering the ground and the first excited states in the length gauge formalism [37]. It has not been studied up to now in what way the latter result, obtained in the case of diatomics, can be applied to a polyatomic molecule. In the present study of HHG in  $\text{C}_{60}$  we will therefore use both the original length gauge formalism as well as the velocity gauge form and compare the results.

The paper is organized as follows. In Sec. II we sketch the SFA formalism for high-harmonic generation in complex molecules, taking into account the geometrical structure of

the molecule and the orbital symmetry. We further introduce a simple model that will allow us to retrieve information about the radius of the fullerene from the high-harmonic spectra. In the next section we will discuss the results of our numerical calculations for high-harmonic generation of  $\text{C}_{60}$  obtained at different wavelengths of the laser field. A comparison between the high-harmonic response for ensembles of aligned and randomly oriented fullerenes will be presented. We will further show how structural information can be gained from the interference pattern in the spectra. The paper ends with a short summary.

## II. THEORY

### A. Strong-field approximation for HHG in complex molecules

In order to evaluate high-harmonic spectra for complex molecules in intense laser pulses we use an extension of the Lewenstein model [35] to the molecular case. We consider the interaction of the active electron with the external field in both the length and the velocity gauges. Using the SAE approximation the time-dependent dipole moment of the molecule can then be written as (Hartree atomic units  $e = m = \hbar = 1$  are used) (e.g., [36])

$$\begin{aligned} \mathbf{D}(\{\mathbf{R}\}_j; t) = & -i \int_0^t dt' \int d^3k \mathbf{d}_{\text{rec}}^*(\mathbf{k} + \mathbf{A}(t), \{\mathbf{R}\}_j) \\ & \times d_{\text{ion}}^{(L)}(\mathbf{k} + \mathbf{A}(t'), \{\mathbf{R}\}_j; t') \exp[-iS(\mathbf{k}, t, t')] + \text{c.c.} \end{aligned} \quad (1)$$

in the length gauge and as

$$\begin{aligned} \mathbf{D}(\{\mathbf{R}\}_j; t) = & -i \int_0^t dt' \int d^3k \mathbf{d}_{\text{rec}}^*(\mathbf{k}, \{\mathbf{R}\}_j) \\ & \times d_{\text{ion}}^{(V)}(\mathbf{k}, \{\mathbf{R}\}_j; t') \exp[-iS(\mathbf{k}, t, t')] + \text{c.c.} \end{aligned} \quad (2)$$

in the velocity gauge.  $S(\mathbf{k}, t, t') = \int_{t'}^t dt'' \{[\mathbf{k} + \mathbf{A}(t'')]^2/2 + I_p\}$  is the semiclassical action,  $I_p$  is the ionization potential of the molecular ground state, and  $\mathbf{A}(t) = -c \int_{-\infty}^t \mathbf{E}(t') dt'$  is the vector potential of the linearly polarized laser field  $\mathbf{E}(t)$ .  $\{\mathbf{R}\}_j$  is a shorthand notation for the coordinates of the nuclei in the molecule. The ionization and recombination amplitudes in Eqs. (1) and (2) are given by

$$d_{\text{ion}}^{(L)}(\mathbf{k}, \{\mathbf{R}\}_j; t) = \langle \phi_0(\mathbf{k}, \mathbf{r}) | \mathbf{E}(t) \cdot \mathbf{r} | \Phi_i(\mathbf{r}, \{\mathbf{R}\}_j) \rangle, \quad (3)$$

$$d_{\text{ion}}^{(V)}(\mathbf{k}, \{\mathbf{R}\}_j; t) = \left( \frac{\mathbf{k} \cdot \mathbf{A}(t)}{c} + \frac{A^2(t)}{2c^2} \right) \times \langle \phi_0(\mathbf{k}, \mathbf{r}) | \Phi_i(\mathbf{r}, \{\mathbf{R}\}_j) \rangle, \quad (4)$$

and

$$\mathbf{d}_{\text{rec}}(\mathbf{k}, \{\mathbf{R}\}_j) = \langle \phi_0(\mathbf{k}, \mathbf{r}) | -\mathbf{r} | \Phi_i(\mathbf{r}, \{\mathbf{R}\}_j) \rangle, \quad (5)$$

respectively.  $\phi_0(\mathbf{k}, \mathbf{r})$  is a plane wave of momentum  $\mathbf{k}$  and  $\Phi_i(\mathbf{r}, \{\mathbf{R}\}_j)$  is the undressed initial-state orbital of the active electron in the molecule. Angular brackets denote integration over the electron coordinate.

We represent the active orbital as a linear combination of atomic orbitals  $\phi_{j,i}(\mathbf{r}, \{\mathbf{R}\}_j)$ , centered at the nuclear positions  $\mathbf{R}_j$ ,  $j = 1, 2, \dots, M$ :

$$\Phi_i(\mathbf{r}, \{\mathbf{R}\}_j) = \sum_{j=1}^M \sum_{l=1}^{l_{\max}} a_{j,l} \phi_{j,l}(\mathbf{r}, \mathbf{R}_j), \quad (6)$$

where  $M$  is the number of the nuclei in the molecule,  $a_{j,l}$  are the variational coefficients of the atomic functions, and  $l_{\max}$  is the size of the basis set used. The dipole moments in Eqs. (1) and (2) therefore take direct account of the multicenter nature of the molecule, its geometrical structure as well as the orbital symmetry. As discussed at the outset, any multi-electron effects as well as transitions to excited states of the molecule are not considered in this formalism. For the present purpose of evaluating high-harmonic spectra in the  $C_{60}$  fullerene, we have acquired its geometrical structure using the density-functional tight-binding method [39–41]. The atomic orbitals are then obtained using the self-consistent Hartree-Fock method with Gaussian basis functions [42].

The spectrum of the emitted light polarized along a certain direction  $\hat{\mathbf{e}}$  is obtained by modulus squaring the Fourier transform of the dipole acceleration,

$$\hat{\mathbf{e}} \cdot \mathbf{a}(\{\mathbf{R}\}_j; \Omega) = \int_0^{T_p} dt \hat{\mathbf{e}} \cdot \ddot{\mathbf{D}}(\{\mathbf{R}\}_j; t) \exp(i\Omega t), \quad (7)$$

where the integration is carried out over the duration of the laser pulse,  $T_p$ , by applying a fast Fourier transform algorithm. The numerical calculation of Eqs. (1) and (2) involves a multidimensional integration over momentum and time. As usual [35], we have performed the three-dimensional integration over  $\mathbf{k}$  using the saddle point or stationary phase method, while all time integrations are performed numerically. Since the intensity of the harmonics is strongest for polarization along the direction of the linearly polarized laser field, we have considered the contribution in this direction only. The orientation of the molecule is determined in Eq. (7) via the coordinates of the nuclei,  $\{\mathbf{R}\}_j$ . In the present work we have performed calculations using ensembles of aligned and randomly oriented  $C_{60}$  fullerenes. The latter are obtained by averaging the modulus squared of the dipole acceleration over the different orientations of the fullerene.

### B. Spherical model

Both recombination and ionization matrix elements are sensitive to the molecular structure and alignment. It has been argued, however, that the interference patterns in small diatomic molecules are dictated primarily by the recombination matrix element [2,6,8,9,13]. We will use the highly symmetric nature of the initial state in  $C_{60}$  to derive an approximate expression for the recombination matrix element. With this formula we will be able to obtain the radius of the fullerene cage from the interference minima in the high-harmonic spectra of  $C_{60}$ .

Writing explicitly the modulus squared of the recombination transition amplitude (5) in a given direction  $\hat{\mathbf{e}}$  we get

$$|\hat{\mathbf{e}} \cdot \mathbf{d}_{\text{rec}}(\mathbf{k}, \{\mathbf{R}\}_j)|^2 \propto \left| \int e^{i\mathbf{k} \cdot \mathbf{r}} \Phi_i(\mathbf{r}, \{\mathbf{R}\}_j) \hat{\mathbf{e}} \cdot \mathbf{r} d\mathbf{r} \right|^2. \quad (8)$$

Since the  $C_{60}$  molecule has almost spherical symmetry, we approximate the initial state  $\Phi_i(\mathbf{r}, \{\mathbf{R}\}_j)$  by a simple spherical-shell-like state as [23]

$$\Phi_i(\mathbf{r}, \{\mathbf{R}\}_j) = \Theta_R(r) Y_{l_i, m_i}(\hat{\mathbf{r}}). \quad (9)$$

where  $Y_{l_i, m_i}$  is a spherical harmonic,  $\mathbf{r} = r\hat{\mathbf{r}}$ , and the radial function  $\Theta_R(r)$  reads

$$\Theta_R(r) = \begin{cases} -V_0, & R - \Delta \leq r \leq R, \\ V_0, & R \leq r \leq R + \Delta, \end{cases} \quad (10)$$

where  $R = \frac{1}{60} \sum_{j=1}^{60} |\mathbf{R}_j| = 6.74$  a.u. and  $\Delta = 0.95$  a.u. [23] are the radius of the spherical shell and the half-width of the shell, respectively, and  $V_0 = 1/2R\Delta^2$ . Using the spherical wave expansion of a plane wave, we can write Eq. (8) as

$$|\hat{\mathbf{e}} \cdot \mathbf{d}_{\text{rec}}(\mathbf{k}, \{\mathbf{R}\}_j)|^2 \propto \left| \sum_{l_f, m_f} Y_{l_f, m_f}^*(\hat{\mathbf{k}}) (-i)^{l_f} \times \int j_{l_f}(kr) \Theta_R(r) r^3 dr \right. \\ \left. \times \int Y_{l_f, m_f}^*(\hat{\mathbf{r}}) \hat{\mathbf{e}} \cdot \hat{\mathbf{r}} Y_{l_i, m_i}(\hat{\mathbf{r}}) d\hat{\mathbf{r}} \right|^2, \quad (11)$$

where  $\mathbf{k} = k\hat{\mathbf{k}}$ . The integral over the angular part leads to a selection rule  $l_f = l_i \pm 1$ . We are interested in the dependence of the matrix element on  $k$  in order to analyze the harmonic spectrum. We therefore further approximate the spherical Bessel functions by trigonometric functions, as in [23]. The angular terms in  $m_f$  and  $m_i$ , which are independent of  $k$ , can then be neglected since they contribute as a constant to the  $k$  dependence of the matrix element. An approximate expression for the recombination matrix element in the case of a fullerene then yields (cf. [23])

$$|\hat{\mathbf{e}} \cdot \mathbf{d}_{\text{rec}}(\mathbf{k}, \{\mathbf{R}\}_j)|^2 \propto \frac{V_0^2}{k^2} \left[ \int_R^{R+\Delta} \cos\left(kr + \alpha_{l_i} - \frac{l_i}{2}\pi\right) r^2 dr \right. \\ \left. - \int_{R-\Delta}^R \cos\left(kr + \alpha_{l_i} - \frac{l_i}{2}\pi\right) r^2 dr \right]^2. \quad (12)$$

Please note that Eq. (12) does not have any angular dependence. Therefore, it can be used only for an analysis of the matrix element and the high-harmonic spectrum as a function of harmonic order but not for alignment dependence.

The  $C_{60}$  initial states are well described by  $l_i=5$  for the HOMO of  $h_u$  symmetry and  $l_i=4$  for the  $h_g$  HOMO-1 and the  $g_g$  HOMO-2. We have used  $\alpha_4=1$  and  $\alpha_5=1.4$ , following the arguments established in Ref. [23]. In the next section we discuss the predictions of this model for the different  $C_{60}$  orbitals and compare them with the interference patterns in the high-harmonic spectrum as well as with the actual recombination matrix elements, used in the full calculations. We further discuss how the above formula can be used to estimate the radius of the fullerene cage from the high-harmonic spectra information.

### III. RESULTS AND DISCUSSION

We have performed calculations for HHG spectra of  $C_{60}$  molecules in intense laser pulses at different wavelengths of the field. The goal of our studies was to identify characteristic interference patterns in the spectra of fullerenes. Furthermore, we intended to analyze how information concerning the geometrical structure of the fullerene can be extracted from the spectra. In all previous studies of HHG of simple molecules it has been found that it is necessary to (partially) align the molecular ensemble to observe interference patterns in the spectra [6,11,12]. In other words, when an ensemble of randomly oriented molecules has been irradiated by laser radiation, all the interference features were “washed out.” Below, we will study ensembles of aligned and randomly oriented fullerenes. It is certainly difficult, if not impossible, to align a  $C_{60}$  molecule in an experiment. Therefore, we consider our results for aligned  $C_{60}$  molecules as a theoretical study, which will allow us to identify the interference patterns. These results will further serve for a comparison with those obtained for the experimentally interesting case of randomly oriented fullerenes.

For the case of aligned  $C_{60}$  molecules, we establish the polarization direction of the laser field as fixed along the main symmetry axis of the fullerene, namely through the center of two opposite pentagons. In Fig. 1 we present a comparison of the results for the high-harmonic spectra at (a) 800 and (b) 1800 nm as a function of the harmonic order. Both spectra have been obtained in the length gauge for a pulse with a peak intensity of  $I_0=5 \times 10^{13}$  W/cm<sup>2</sup>, a pulse duration of 30 fs, and a  $\sin^2$  pulse shape. The peak intensity has been chosen to be close to but below the corresponding saturation intensity of the neutral fullerene for both wavelengths.

It is seen from the results that the cutoff of the HHG spectra is in good agreement with the predictions of the semiclassical three-step model (marked by the arrows). There is obviously no unphysical extension of the plateau, as has been found in numerical simulations using the length gauge for diatomics with large internuclear distances [36]. We therefore suppose that application of the length gauge formulation of the Lewenstein model to the fullerene case at the present laser parameters is suitable. While the spectra at 800 nm do not show any specific modulation due to the short plateau [Fig. 1(a)], we observe characteristic modulations in the strengths of the harmonics in the plateau at 1800 nm driving wavelengths [Fig. 1(b)]. A small minimum is seen in the region of the 37th to 41st harmonics and a second pronounced one at the 69th and 71st harmonics. We expect that these minima are due to interference effects from the multi-center nature of the  $C_{60}$  molecule. As discussed at the outset, similar structures have been observed before in other aligned di- and polyatomic molecules too, and interpreted as due to interferences between the dipole amplitudes arising from the recombination of the electron into the ground state [6,8,10–13].

In order to test our expectation we have plotted in Fig. 1(c) the modulus squared of the recombination matrix element, Eq. (5), as a function of the harmonic order (solid line). To this end we have used the relation  $n\omega_{1800}=k^2/2$

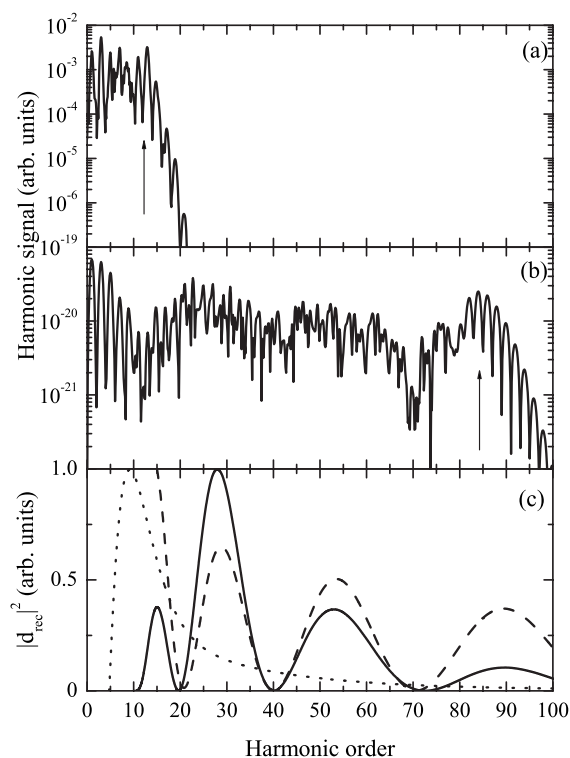


FIG. 1. HHG spectra for an ensemble of aligned  $C_{60}$  molecules at  $\lambda =$  (a) 800 and (b) 1800 nm and a peak laser intensity of  $I_0=5 \times 10^{13}$  W/cm<sup>2</sup>, a pulse duration of 30 fs, and a  $\sin^2$  pulse shape. The spectra are obtained for the  $h_u$  HOMO in length gauge; the arrows indicate the cutoff of the plateau as predicted from the semiclassical model [35]. (c) Recombination matrix element as obtained from the full calculation (solid line), the incoherent sum of the contributions from the atomic centers (dotted line), and the spherical model (dashed line). For the presentation of the recombination matrix element as a function of the harmonic order  $n$ , we have used the relation  $n\omega_{1800}=k^2/2+I_p$  with frequency  $\omega_{1800}=0.0253$  a.u. ( $\lambda = 1800$  nm) and  $I_p=0.272$  a.u.

+ $I_p$  with  $\omega_{1800}=0.0253$  a.u. ( $\lambda=1800$  nm). One sees a clear correlation between the zeros in the recombination matrix element and the position of the minima in the harmonic spectrum at 1800 nm in panel Fig. 1(b). In additional test calculations, we have deliberately neglected the interference effects in the recombination matrix element by modulus squaring the partial contributions from each of the 60 atomic centers and then calculating the sum. The result obtained is presented as a dotted line in Fig. 1(c). Please note the absence of the interference patterns in the results obtained from these incoherent calculations (dotted line), which confirms the origin of the minima in the HHG spectrum at 1800 nm as a multislit interference phenomenon.

The characteristic minima should therefore contain information about the geometric structure and the symmetry of the active orbital of the fullerene. To get more insight in the origin we compare in Fig. 1(c) the predictions of the spherical model Eq. (12) (dashed line) with those of the full recombination matrix element (solid line). In spite of the crude approximation for the initial and final states in the spherical model, there is good agreement in the positions of the minima with the results of the full calculations. Similar con-

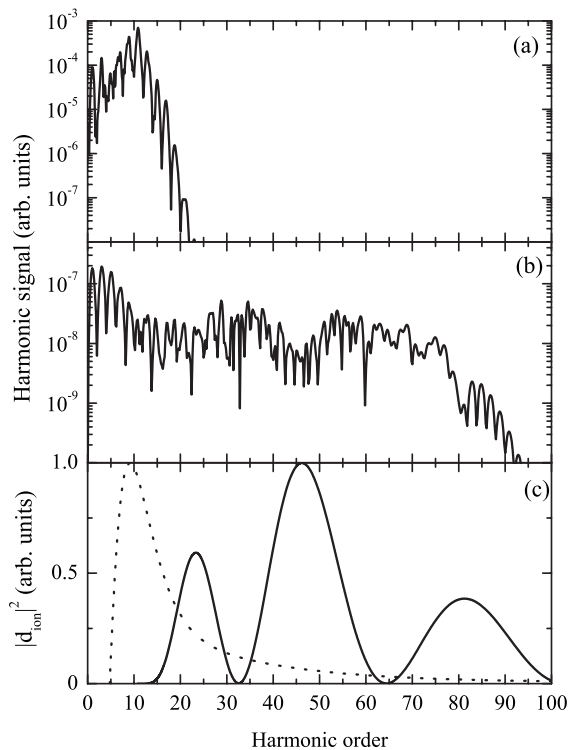


FIG. 2. HHG spectra at  $\lambda =$  (a) 800 and (b) 1800 nm using the velocity gauge. The other parameters are as in Fig. 1. (c) Ionization matrix element as a function of the harmonic order. Solid line, full calculation; dotted line, incoherent sum of the partial contributions.

clusions have been reached before for photoelectron spectra of  $C_{60}$  interacting with weak synchrotron radiation [23]. This leads us to the assumption that the simple spherical model incorporates the main parameters of the multislit interference phenomenon. The position of the minima in the HHG spectra therefore depends on the symmetry of the active orbital, namely, on the value of the angular momentum  $l_i$  in the spherical model, as well as the radius of the atomic cage,  $R$ , and the thickness of the electronic cloud,  $\Delta$ .

The results from the recombination matrix elements and the analysis using the simple spherical models may further establish a way to retrieve the actual radius of the fullerene via the high-harmonic spectrum. This option may be interesting in view of recent experimental observations and theoretical predictions of oscillations of the nuclear frame during the interaction of  $C_{60}$  with an intense laser pulse [43,44]. Assuming  $l_i$  and  $\Delta$  as fixed, the radius  $R$  can be obtained from the positions of the minima in the harmonic spectra by solving Eq. (12) numerically. Taking  $n_1=39$  and  $n_2=70$  as the positions of the two minima in the present harmonic spectrum, we find numerical values for the radius of the shell (fullerene) as  $R_1=6.48$  a.u. and  $R_2=6.26$  a.u., which are in rough agreement with the average distance of the atoms from the center in the present LCAO initial state ( $R=6.74$  a.u.).

Before proceeding we stress that the interpretation given above is most stringent using the results obtained in the length gauge. This is seen immediately from the results for the HHG spectra obtained in the velocity gauge, which are shown in Figs. 2(a) and 2(b). For the calculations we have

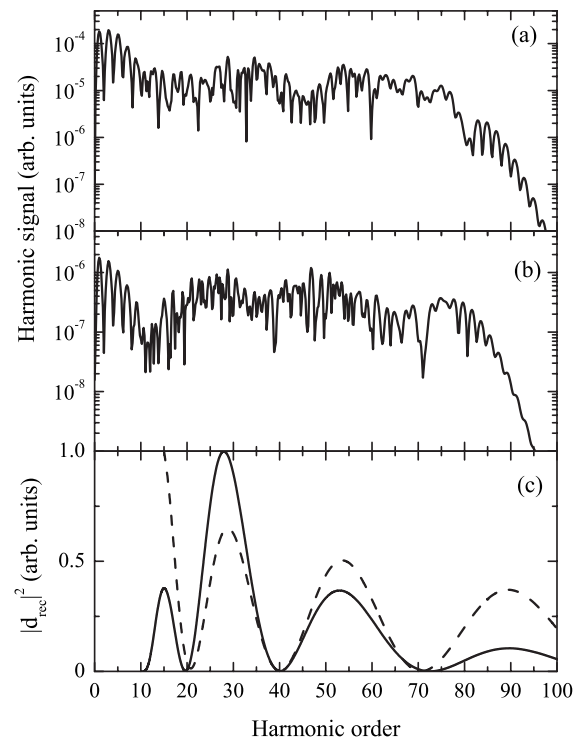
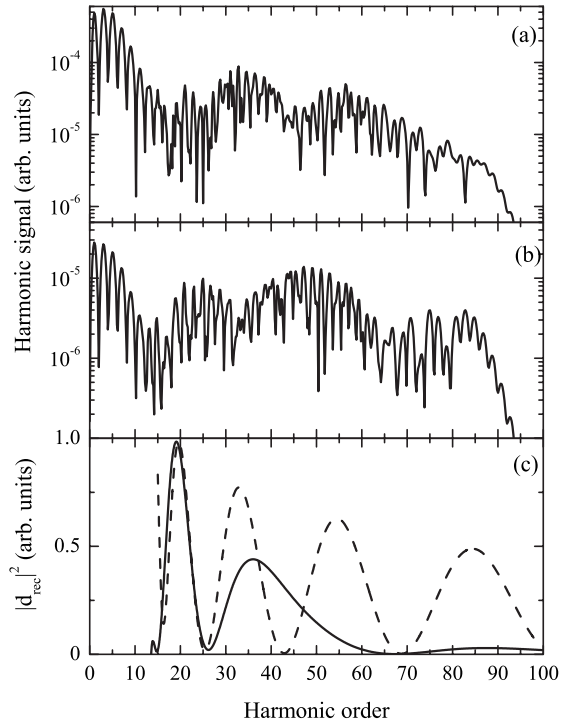


FIG. 3. High-harmonic spectrum for an ensemble of randomly oriented  $C_{60}$  molecules ( $h_u$  HOMO) using (a) the velocity and (b) the length gauge. Laser parameters are as in Fig. 1(b). (c) Comparison of the corresponding recombination matrix elements obtained from the full calculation (solid line) and from the spherical model (dashed line).

used the same alignment of the  $C_{60}$  molecule with respect to the polarization direction and the same laser parameters. Clearly, the plateaus of both spectra extend to the same orders as in the length gauge calculations, but the characteristic modulation in the spectrum obtained at 1800 nm does not agree with the modulations seen in Fig. 1(b). Furthermore, in the results obtained in the velocity gauge the position of the minimum at about  $n=45$  is determined by neither the recombination [cf. Fig. 1(c)] nor the ionization matrix element [Fig. 2(c)]. We may, however, point out that in both spectra, obtained in the length as well as the velocity gauge, we observe interference patterns. Despite the fact that the positions of the minima in the spectra do vary, we expect that the general structure should be observable. Similar discrepancies between the results obtained in the two gauges have been found before for other molecules too (cf. [2]).

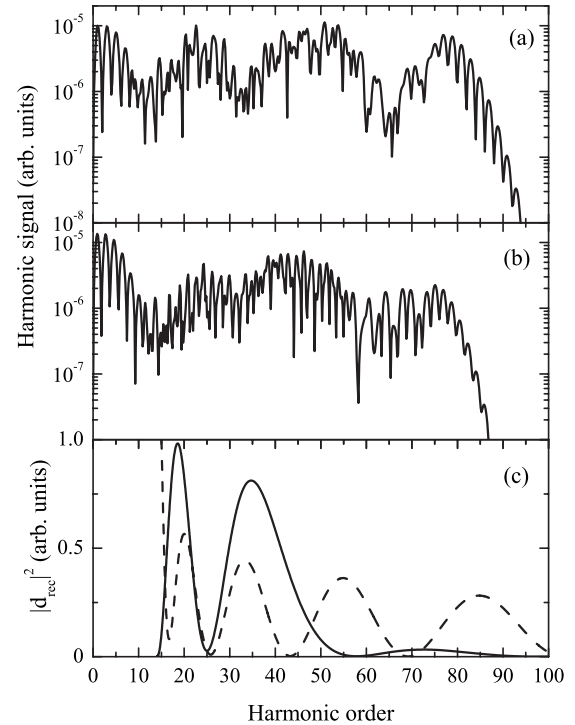
Do the interference minima in the harmonic spectra still show up for the experimentally relevant case of an ensemble of randomly oriented fullerenes? To answer this question we have calculated the harmonic spectra for different orientations of the fullerene and averaged the results. The respective HHG spectra obtained at the longer wavelength in (a) velocity gauge and (b) length gauge are shown in Fig. 3. Also shown in Fig. 3(c) are the recombination matrix element for the case of random orientation of the fullerene (solid line) and the prediction of the spherical model (dashed line). It is seen from the figure that the modulations in the HHG spectra are still present although the positions of the minima are


 FIG. 4. Same as Fig. 3 but for the  $h_g$  HOMO-1.

slightly shifted as compared to the results obtained for the aligned configuration. The presence of interference minima in the case of randomly oriented molecules has not been observed for the previously investigated di- and polyatomic species and is clearly due to the highly symmetric geometry of the fullerene and should be characteristic for all molecules with such a geometry.

As discussed above, the interference patterns in the HHG spectra can be interpreted, at least in the length gauge, as due to the geometry of the atomic cage and the symmetry of the molecular orbital. It is therefore illustrative to investigate how the HHG spectra change if molecular orbitals of other symmetries are used. In Figs. 4 and 5 we therefore present the spectra and the recombination matrix elements for the HOMO-1 ( $h_g$  symmetry,  $l_i=4$ ) and HOMO-2 ( $g_g$  symmetry,  $l_i=4$ ), respectively. We have assumed random orientation of the fullerene, and the laser parameters were the same as in Fig. 3.

Like the results for the  $h_u$  HOMO, the HHG spectra obtained for the two inner valence shells show clear minima in the plateau region; however, the positions of the minima do not agree for the two gauges. We may note that these minima are due to the multislit interference effect too, since they disappear in test calculations in which the contributions from the different atomic center are added incoherently (not shown). Furthermore, the minima are clearly present although random orientation of the fullerene has been assumed in the calculations. As before, the positions of the minima in the length gauge calculation [Figs. 4(b) and 5(b)] do match with the zeros in the recombination matrix element [solid line in Figs. 4(c) and 5(c)]. On the other hand, there is an agreement between the first minimum in the HHG spectra and that of the spherical model [dashed line in Figs. 4(c) and 5(c)], but not for the second one.


 FIG. 5. Same as Fig. 3 but for the  $g_g$  HOMO-2.

#### IV. CONCLUSIONS

We have calculated high-order harmonic generation in  $C_{60}$  molecules interacting with a linearly polarized intense laser pulse using the strong-field approximation. To this end we have extended the so-called three-step or Lewenstein model, to the case of a molecule, using molecular wave functions which take account of the positions of the nuclei as well as the symmetry of the active orbital. Calculations are performed in the length as well as the velocity gauge for different wavelengths and several active orbitals of the fullerene.

The results show modulations in the plateaus of the high-harmonic spectra obtained at mid-infrared wavelengths. Such patterns do not occur at wavelengths in the near-infrared regime due to the short plateau extension at intensities below the saturation level. The patterns are found to be due to a multislit interference effect between the contributions from the different atomic centers to the total dipole moment. Unlike in the case of di- and other polyatomics, the interference patterns do not disappear for molecular ensembles oriented randomly with respect to the polarization axis of the laser. This is due to the high symmetry of the nuclear cage of the  $C_{60}$  molecule. The modulations are found in the results obtained in both the length as well as the velocity gauge; the positions of the interference minima, however, do not agree with each other in the two gauges.

The results obtained in the length gauge have been further analyzed by comparing the positions of the interference minima with the zeros of the recombination matrix element. Good agreement has been found for the full calculation as well as with a simple spherical model calculation for the first valence orbital ( $h_u$  HOMO). It has been shown how the latter

model can be used to obtain information about the geometry of the fullerene in the laser pulse from the interference pattern in the harmonic spectra. It is expected that the observed oscillations and multislit interference effect will appear for

other molecules having a nearly spherical structure with a large radius too. Therefore the observation of high-harmonic spectra may be a useful tool to identify structural changes in such complex molecules induced by an intense laser pulse.

- 
- [1] A. H. Zewail, *Science* **242**, 1645 (1988).  
 [2] M. Lein, *J. Phys. B* **40**, R135 (2007).  
 [3] P. B. Corkum, *Phys. Rev. Lett.* **71**, 1994 (1993).  
 [4] K. J. Schafer, B. Yang, L. F. DiMauro, and K. C. Kulander, *Phys. Rev. Lett.* **70**, 1599 (1993).  
 [5] P. B. Corkum and F. Krausz, *Nat. Phys.* **3**, 381 (2007).  
 [6] M. Lein, N. Hay, R. Velotta, J. P. Marangos, and P. L. Knight, *Phys. Rev. Lett.* **88**, 183903 (2002).  
 [7] S. Ramakrishna and T. Seideman, *Phys. Rev. Lett.* **99**, 113901 (2007).  
 [8] M. Lein, N. Hay, R. Velotta, J. P. Marangos, and P. L. Knight, *Phys. Rev. A* **66**, 023805 (2002).  
 [9] C. Figueira de Morisson Faria, *Phys. Rev. A* **76**, 043407 (2007).  
 [10] T. Kanai, S. Minemoto, and H. Sakai, *Nature (London)* **435**, 470 (2005).  
 [11] C. Vozzi *et al.*, *Phys. Rev. Lett.* **95**, 153902 (2005).  
 [12] R. Torres *et al.*, *Phys. Rev. Lett.* **98**, 203007 (2007).  
 [13] J. Itatani, J. Levesque, D. Zeidler, H. Niikura, H. Pépin, J. C. Kieffer, P. B. Corkum, and D. M. Villeneuve, *Nature (London)* **432**, 867 (2004).  
 [14] R. Santra and A. Gordon, *Phys. Rev. Lett.* **96**, 073906 (2006).  
 [15] R. Santra, *Chem. Phys.* **329**, 357 (2006).  
 [16] W. H. E. Schwarz, *Angew. Chem.* **45**, 1508 (2006).  
 [17] S. Patchkovskii, Z. Zhao, T. Brabec, and D. M. Villeneuve, *Phys. Rev. Lett.* **97**, 123003 (2006).  
 [18] S. Patchkovskii, Z. X. Zhao, T. Brabec, and D. M. Villeneuve, *J. Chem. Phys.* **126**, 114306 (2007).  
 [19] J. Levesque, D. Zeidler, J. P. Marangos, P. B. Corkum, and D. M. Villeneuve, *Phys. Rev. Lett.* **98**, 183903 (2007).  
 [20] V.-H. Le, A.-T. Le, R.-H. Xie, and C. D. Lin, *Phys. Rev. A* **76**, 013414 (2007).  
 [21] T. Liesch, O. Plotzke, F. Heiser, U. Hergenhahn, O. Hemmers, R. Wehlitz, J. Viefhaus, B. Langer, S. B. Whitfield, and U. Becker, *Phys. Rev. A* **52**, 457 (1995).  
 [22] Y. B. Xu, M. Q. Tan, and U. Becker, *Phys. Rev. Lett.* **76**, 3538 (1996).  
 [23] S. Hasegawa, T. Miyamae, K. Yakushi, H. Inokuchi, K. Seki, and N. Ueno, *Phys. Rev. B* **58**, 4927 (1998).  
 [24] A. Rudel, R. Hentges, U. Becker, H. S. Chakraborty, M. E. Madjet, and J. M. Rost, *Phys. Rev. Lett.* **89**, 125503 (2002).  
 [25] S. Korica, D. Rolles, A. Reinköster, B. Langer, J. Viefhaus, S. Cvejanović, and U. Becker, *Phys. Rev. A* **71**, 013203 (2005).  
 [26] O. Franck and J. M. Rost, *Chem. Phys. Lett.* **271**, 367 (1997).  
 [27] A. Jaroń-Becker, A. Becker, and F. H. M. Faisal, *Phys. Rev. Lett.* **96**, 143006 (2006).  
 [28] A. Jaroń-Becker, A. Becker, and F. H. M. Faisal, *J. Chem. Phys.* **126**, 124310 (2007).  
 [29] S. Chelkowski, A. Conjusteau, T. Zuo, and A. D. Bandrauk, *Phys. Rev. A* **54**, 3235 (1996).  
 [30] D. G. Lappas and J. P. Marangos, *J. Phys. B* **33**, 4679 (2000).  
 [31] W. Qu, Z. Chen, Z. Xu, and C. H. Keitel, *Phys. Rev. A* **65**, 013402 (2001).  
 [32] M. Lein, P. P. Corso, J. P. Marangos, and P. L. Knight, *Phys. Rev. A* **67**, 023819 (2003).  
 [33] G. Lagmago Kamta and A. D. Bandrauk, *Phys. Rev. A* **70**, 011404(R) (2004).  
 [34] G. L. Kamta and A. D. Bandrauk, *Phys. Rev. A* **71**, 053407 (2005).  
 [35] M. Lewenstein, P. Balcou, M. Y. Ivanov, A. L'Huillier, and P. B. Corkum, *Phys. Rev. A* **49**, 2117 (1994).  
 [36] C. C. Chirilă and M. Lein, *Phys. Rev. A* **73**, 023410 (2006).  
 [37] J. Chen, S.-I. Chu, and J. Liu, *J. Phys. B* **39**, 4747 (2006).  
 [38] R. Kopold, W. Becker, and M. Kleber, *Phys. Rev. A* **58**, 4022 (1998).  
 [39] D. Porezag, T. Frauenheim, T. Kohler, G. Seifert, and R. Kaschner, *Phys. Rev. B* **51**, 12947 (1995).  
 [40] G. Seifert, D. Porezag, and T. Frauenheim, *Int. J. Quantum Chem.* **58**, 185 (1996).  
 [41] M. Elstner, D. Porezag, G. Jungnickel, J. Elsner, M. Haugk, T. Frauenheim, S. Suhai, and G. Seifert, *Phys. Rev. B* **58**, 7260 (1998).  
 [42] Computer code GAUSSIAN03, Revision C.02 (Gaussian, Inc., Wallingford, CT, 2004), <http://www.gaussian.com>  
 [43] R. Sahnoun, K. Nakai, Y. Sato, H. Kono, Y. Fujimara, and M. Tanaka, *Chem. Phys. Lett.* **430**, 167 (2006).  
 [44] T. Laarmann, I. Shchatsinin, A. Stalmashonak, M. Boyle, N. Zhavoronkov, J. Handt, R. Schmidt, C. P. Schulz, and I. V. Hertel, *Phys. Rev. Lett.* **98**, 058302 (2007).